

Quantum Chemical Computational Studies on Magnetic Properties of Different 2D Metal Organic Frameworks

¹Md Asif Amin

¹Assistant Professor

¹Department of Chemistry,

¹Balurghat Mahila Mahavidyalaya, Balurghat-733101, India

Abstract : 2D metal organic framework has advantages over graphene based structure due to stability and different properties which enhances application of such materials as spin filters and spin injectors. In this review we focuses on quantum computational studies on different types of half metallic compounds. Introduction of transition metals gives rise to some interesting properties.

IndexTerms - Half metal, Metal Organic Frameworks, Computation.

I. INTRODUCTION

Half metallic magnets, which display a metallic density of states (DOS) for one spin component but are insulating or semiconducting for the other, have promising applications in spintronic devices as spin filters and spin injectors.^[1,2] Thus, much research effort has been devoted to the search for novel materials with robust half-metallic properties. When compared to transition metal-containing compounds, such as manganese perovskites,^[3] Heusler alloys^[4] and dilute magnetic semiconductors,^[5] half-metallic graphene-based materials appear more attractive because of the long spin coherence length in carbon and their compatibility with the maturing graphene technological area.^[6,7] Although a half-metallic DOS has been predicted for zigzag graphene nanoribbons in the presence of a electric field or when their edges are modified by appropriate organic functional groups,^[8,9] the prohibitively large electric field and the fine control of the positions of functional groups make the experimental synthesis of these materials highly improbable.

This review focuses on the theoretical study of the magnetic properties of magnetic systems, that is, on the accurate theoretical computation and proper rationalization of the magnetic properties of magnetic systems using Quantum Chemical methods. Graphene possesses such kind of electronic and magnetic properties and many novel works have been done to investigate those properties. The edge-induced magnetism of graphene nano-ribbons (GNRs) has been found to be highly unstable at room temperature, thus making it difficult for spintronics applications under ambient conditions. Using first-principles calculations, a method has been proposed to overcome this problem by embedding transition-metal atoms into functionalized GNRs. Due to low or vanishing reaction barriers, 3d transition-metal atoms can be easily embedded into GNR once they are functionalized by -F or -CN groups. A systematic study of these materials shows fascinating magnetic properties; Co-embedded systems not only have high magnetic anisotropy energies hundreds of times larger than that of pure GNR and bulk Co, but also, the magnetic preferential directions can be switched by an electric field. Mn-embedded systems exhibit giant magnetic moments and half-metallicity with greatly enhanced stability. Under a small amount of biaxial strain, the magnetic moment of every Mn atom in such a Mn-embedded system can be increased by $2.1\mu_B$ due to a change in the d_{xy} orbital occupancy, and its Curie temperature is estimated to be over 1000 K.^[10]

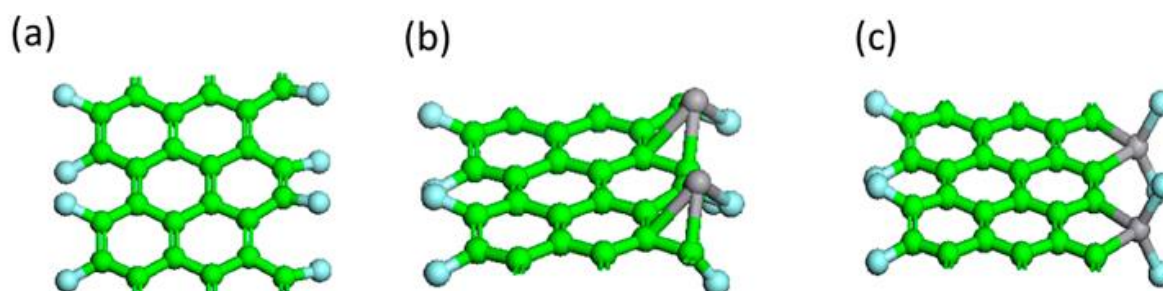


Fig 1: The geometric structure of (a) FAGNR, (b) FAGNR-M, and (c) AGNR-M-F. Green, blue, and gray spheres denote C, N, and M atoms, respectively. AGNR=armchair edge graphene nanoribbons, F=fluorine, M=metal.

II. 2D CARBON NITRIDE

Recently one intriguing functional carbon material with an extended framework has been synthesized by trimerization of a nitrile-containing anion^[11]. This can be considered as asym-triazine structural unit connected by carbon atoms. Such a new type of two-dimensional (2D) graphitic carbon nitride ($g-C_4N_3$) material has been predicted to possess an intrinsic half-metallicity by first-principles calculations^[11]. It was found that the ground state of the primitive (1×1) $g-C_4N_3$ cell is spin-polarized with a magnetic moment of $1 \mu_B$ per unit cell and that the (2×2) reconstruction further enhances its half-metallic characteristics. Clearly, the magnetism of $g-C_4N_3$ does not originate from d or f electrons, thus it is quite interesting to explore what is the driving force for the occurrence of spin polarization in this sp-material.

Polymeric graphitic carbon nitride materials have attracted increasing attention in recent years owing to their potential applications in energy conversion, environment protection, and so on. Here, from first-principles calculations, the electronic structure modification of graphitic carbon nitride ($g-C_3N_4$) in response to carbon doping. Each dopant atom can induce a local magnetic moment of $1.0 \mu_B$ in non-magnetic $g-C_3N_4$. At a doping concentration of $1/14$, the local magnetic moments of the most stable doping configuration which has the dopant atom at the centre of the heptazine unit prefer to align in a parallel way leading to long-range ferromagnetic (FM) ordering. When the joint N atom is replaced by a C atom, the system favours an antiferromagnetic (AFM) ordering in an unstrained state, but can be tuned to ferromagnetism (FM) by applying biaxial tensile strain. More interestingly, the FM state of the strained system is half-metallic with abundant states at the Fermi level in one spin channel and a band gap of 1.82 eV in another spin channel. The Curie temperature (T_c) was also evaluated using a mean-field theory and Monte Carlo simulations within the Ising model. Such tuneable electron spin-polarization and ferromagnetism are quite promising for the applications of graphite carbon nitrides in spintronics.^[11]

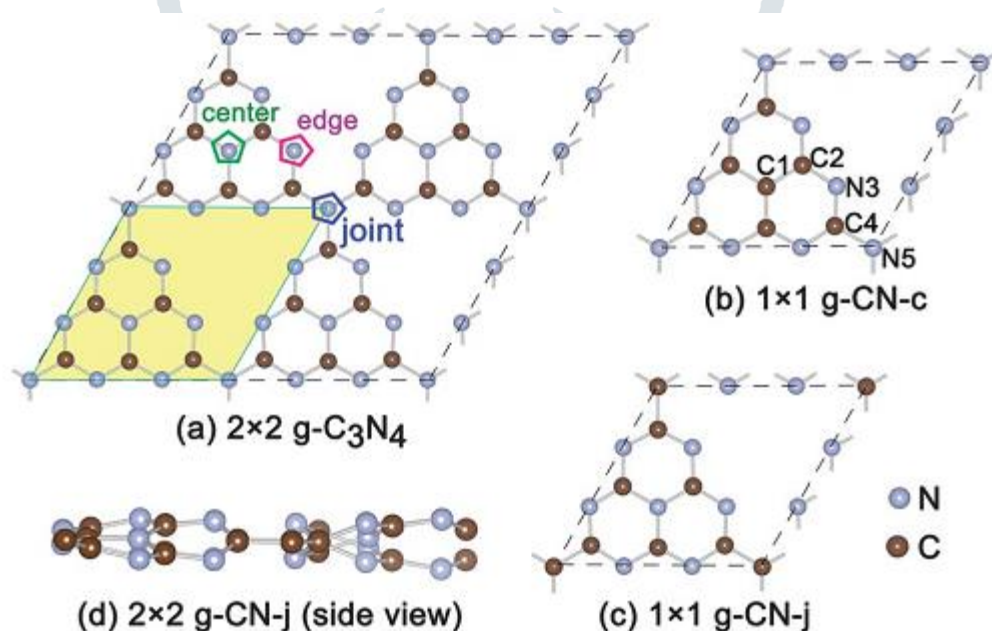


Fig 2: (a) 2×2 Supercell of graphitic carbon nitride based on heptazine ($g-C_3N_4$). Three different types of nitrogen atoms are labelled in this figure. The light yellow region represents a unit cell. (b) The 1×1 unit cell of $g-CN-c$ which is formed by replacing the centre nitrogen atom with a carbon atom. (c) The 1×1 unit cell of $g-CN-j$ with the joint nitrogen atom being substituted with a carbon atom. (d) Side view of the reconstructed 2×2 supercell of $g-CN-j$.

This type of work also has been done with 2D boron allotrope. It has been widely accepted that planar boron structures, composed of triangular and hexagonal motifs are the most stable two-dimensional (2D) phases and likely precursors for boron nanostructures. Recently proposed α -sheet structure and its analogues are identified for the first time to have a distorted Dirac cone, after graphene and silicene the third elemental material with massless Dirac fermions. The buckling and coupling between the two sublattices not only enhance the energetic stability, but also are the key factors for the emergence of the distorted Dirac cone.^[13]

III. COVALENT ORGANIC FRAMEWORKS

The emerging theme of materials genome inspires exciting opportunities to computationally design novel materials with desired properties. Meanwhile, advances on synthetic chemistry and nanotechnology have shown the potential in producing complex

2D lattice that is covalent organic frameworks (COFs). Keeping the above two ingredients in mind, computationally a new family of Organic Topological Insulators (OTIs) have been designed. Organometallic compounds have been looked as molecular building blocks, which consist of C-C and C-metal bonds. To verify the first condition choices are narrowed down to the triphenyl-metal compounds with one metal atom bonded symmetrically to three benzene rings, so that they can be readily self-assembled into a hexagonal lattice, as shown in Fig. 3. To satisfy the second condition, heavy metal atoms have been chosen, such as Pb and Bi, with strong spin orbit coupling (SOC).

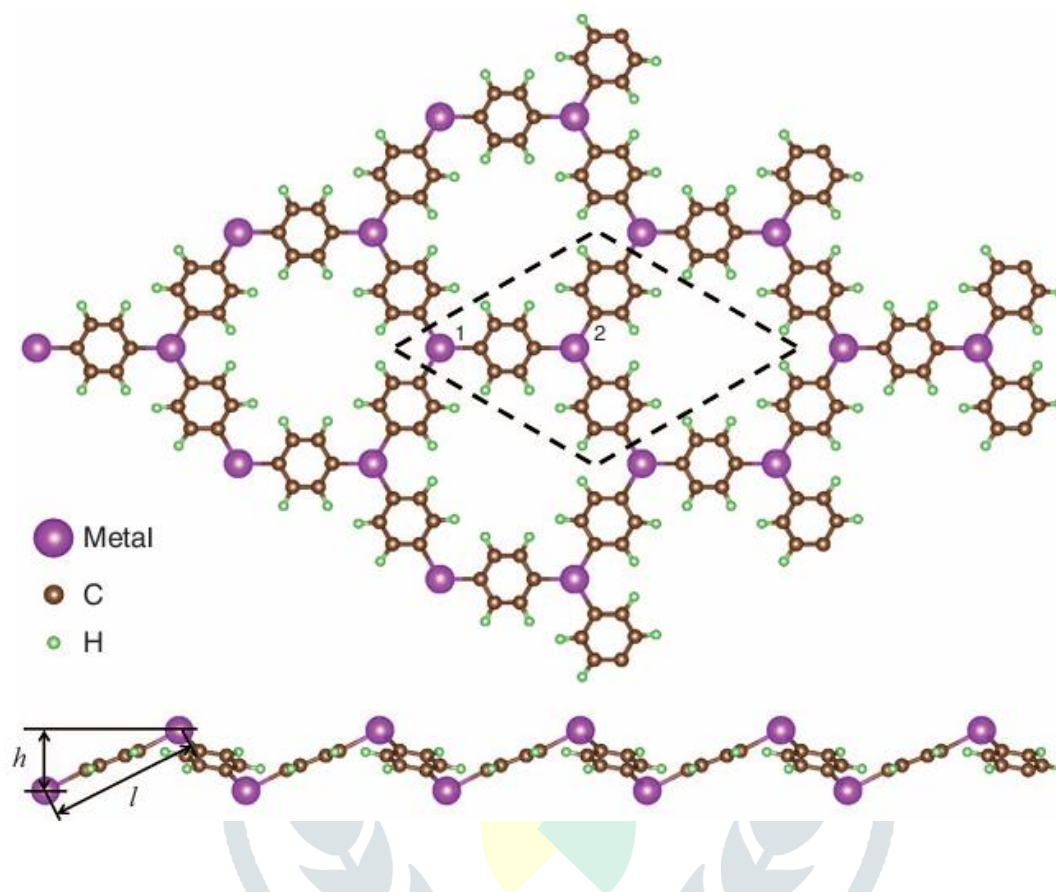


Fig 3: Top and side view of the 2D organometallic superlattice. Dashed lines show the unit cell and the two metal atoms are labelled with 1 and 2. l and h are the distance and height difference between the two metal atoms.

The electronic band structure of 2D triphenyl-lead (TL) lattice displays a Dirac cone at the K point, with the Fermi level located exactly at the Dirac point without SOC. Turning on the SOC, a gap of $\sim 8.6\text{meV}$ opens at the K point. Metals with larger SOC are used to increase the gap. For example, the electronic and topological properties of triphenyl-bismuth (TB) $[\text{Bi}(\text{C}_6\text{H}_5)_3]$ lattice are calculated by replacing Pb with Bi. The stability and structural properties of TB lattice are similar to the TL lattice. It has all the required electronic and topological properties for a TI and a Dirac-cone gap as large as $\sim 43\text{meV}$. However, its Fermi level is $\sim 0.31\text{eV}$ above the Dirac point without SOC because Bi has two extra electrons than Pb. It is worth noting that the OTIs demonstrated here represent a real material system that realizes the Kane-Mele model of 2D TI with a sizable gap, comparable to the known inorganic 2D TI of HgTe quantum well.^[14-16]

IV. HALF METALLIC ANTIFERROMAGNETICS

Half metallic antiferromagnets^[17], a new system with full spin polarization of the conduction electrons, but with any net magnetization, were theoretically predicted in alloys, perovskite oxides, and diluted magnetic semiconductors^[17-19]. The half metals with full electron spin polarization and the diluted magnetic semiconductors^[20] are the most important candidates for application in spintronic materials. If the conduction and valence band edges touch at the Fermi level [Fig 4], this represents a comparatively new class of solids, namely, the gapless semiconductors (GS)^[21]. No threshold energy is required to move electrons from occupied

states to empty states; thus the gapless semiconductors have unique properties as their band structures are extremely sensitive to external influences, e.g., pressure or magnetic field. The electron mobility of a GS is two to four orders of magnitude higher than the mobility of classical semiconductors.

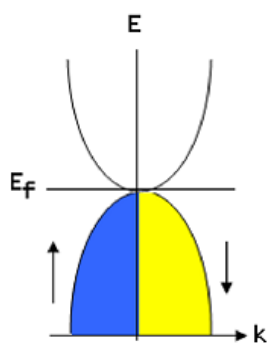


Fig 4: Energy band diagrams for a direct gapless semiconductor with parabolic dispersion between energy and momentum

V. AMMINE BASED MOFS

Recently it was found reaction of 2,3,6,7,10,11-hexaaminotri-phenylene with Ni^{2+} in aqueous NH_3 solution under aerobic conditions produces $\text{Ni}_3(\text{HITP})_2$ (HITP = 2,3,6,7,10,11-hexaiminotriphenylene), a new two-dimensional metal-organic framework (MOF). The new material can be isolated as a highly conductive black powder or dark blue-violet films. Two-probe and van der Pauw electrical measurements reveal bulk (pellet) and surface (film) conductivity values of 2 and $40 \text{ S}\cdot\text{cm}^{-1}$, respectively, both records for MOFs and among the best for any coordination polymer [22]

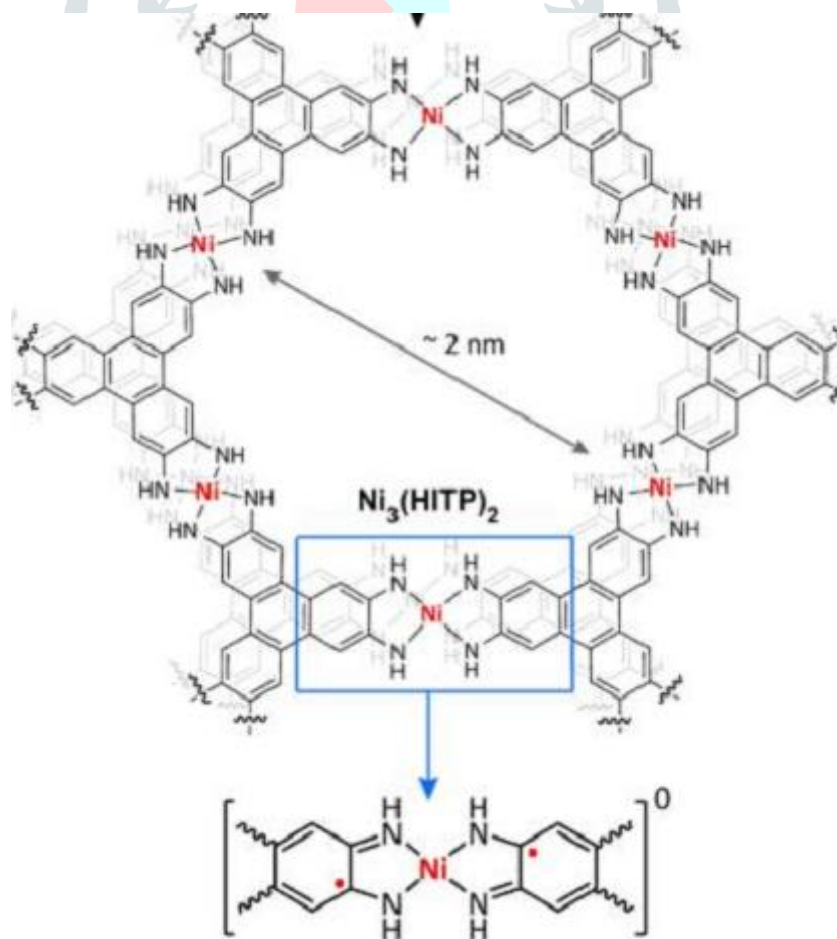


Fig 5: Structure of $\text{Ni}_3(\text{HITP})_2$

VI. PERIODIC 2D MOFs

On-surface polymerisation also used to synthesize periodic system. On-surface polymerization represents a novel bottom-up approach for producing macromolecular structures. To control the on-surface polymerization process a strategy of metal-directed template has been used. A bifunctional compound which contains pyridyl and bromine end groups as the precursor has been chosen. Linear template afforded by pyridyl–Cu–pyridyl coordination effectively promoted Ullmann coupling of the monomers on an Au (111) surface. Taking advantage of efficient topochemical enhancement owing to the conformation flexibility of the Cu–pyridyl bonds, macromolecular porphyrin structures that exhibit a narrow size distribution were synthesized. Scanning tunnelling microscopy and kinetic Monte Carlo simulation used to gain insights into the metal-directed polymerization at the single molecule level. The results reveal that the polymerization process profited from the rich chemistry of Cu which catalyzed the C–C bond formation, controlled the size of the macromolecular products, and organized the macromolecules in a highly ordered manner on the surface.^[23]

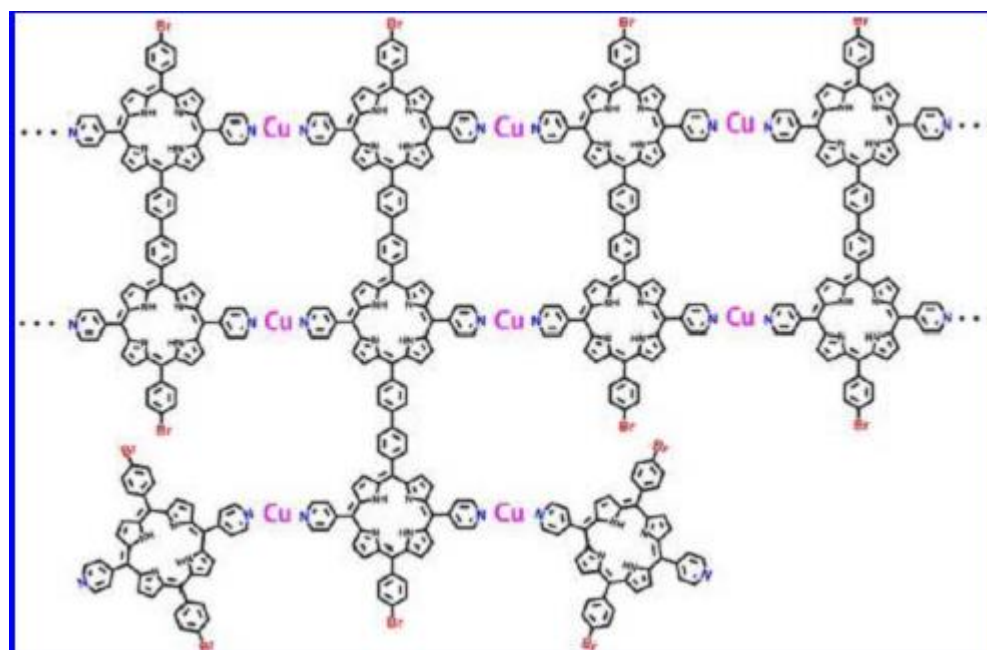


Fig 6: Pyridyl-Cu-Pyridyl structure

VII. ACKNOWLEDGMENT

M.A.A thanks Balurghat Mahila Mahila Mahavidyalaya for all kind of supports.

REFERENCES

- [1] Katsnelson, M. I., Irkin, V. Y., Chioncel, L., Liechtenstein, A. I. and De Groot R. A. 2008. Half-metallic ferromagnets: From band structure to many-body effects. *Review of Modern Physics*, 80: 315.
- [2] Coey J. M. D. and Sanvito S. 2004. Magnetic semiconductors and half-metals. *Journal of Physics D: Applied Physics*, 37; 988.
- [3] Park, J. H., Vescovo, E., Kim, H. J., Kwon, C., Ramesh R. and Venkatesan, T. 1998. Direct evidence for a half-metallic ferromagnet. *Nature*, 392 (6678): 794-796.
- [4] de Groot, R. A., Mueller, F. M., van Engen, P. G. and Buschow, K. H. J. 1983. New Class of Materials: Half-Metallic Ferromagnets. *Physical Review Letters*, 50: 2024.
- [5] Medvedeva, J. E., Freeman, A. J., Cui, X. Y., Stampfl, C. and Newman, N. 2005. Half-Metallicity and Efficient Spin Injection in AlN/GaN:Cr (0001) Heterostructure. *Physical Review Letters*, 94: 146602.
- [6] Dlubak, B., Martin, M. B., Deranlot, C., Servet, B., Xavier, S., Mattana, R., Sprinkle, M., Berger, C., de Heer, W. A., Petroff, F., Anane, A., Seneor P., and Fert, A. 2012. Highly efficient spin transport in epitaxial graphene on SiC. *Nature Physics*, 8: 557-561.
- [7] Biswas, C. and Lee, Y. H. 2011. Graphene Versus Carbon Nanotubes in Electronic Devices. *Advanced Functional Materials*, 21: 3807.
- [8] Son, Y. W., Cohen, M. L. and Louie, S. G. 2006. Half-metallic graphene nanoribbons. *Nature*, 444: 347-349.
- [9] Kan, E., Li, Z., Yang J. and Hou, J. G. 2008. Half-Metallicity in Edge-Modified Zigzag Graphene Nanoribbons. *Journal of the American Chemical Society*, 130 (13): 4224–4225.
- [10] Wu, M., Xeng, X. C., Jena, P. 2013. Unusual Magnetic Properties of Functionalized Graphene Nanoribbons. *Journal of Physical Chemistry Letters*, 4 (15): 2482–2488.
- [11] Lee, J. S., Wang, X. Q., Luo, H. M. and Dai, S. 2010. Fluidic Carbon Precursors for Formation of Functional Carbon under Ambient Pressure Based on Ionic Liquids. *Advanced Materials*, 22 (9): 1004-1007.
- [12] Zhang, X., Zhao, M., Wang, A., Wang, X. and Du, A. 2013. Spin-polarization and ferromagnetism of graphitic carbon nitride materials. *Journal of Materials Chemistry C*, 1: 6265-6270.

- [13] Zhou, X. F., Dong, X., Oganov, A. R., Tian, Y. and Wang, H. T. 2014. Semimetallic Two-Dimensional Boron Allotrope with Massless Dirac Fermions. *Physical Review Letters*, 112 (8): 085502.
- [14] Wang, Z. F., Liu, Z. and Liu, F. 2013. Organic topological insulators in organometallic lattices. *Nature Communications*, 4: 1471.
- [15] Bernevig, B. A., Hughes, T. L. and Zhang, S. C. 2006. Quantum spin hall effect and topological phase transition in HgTe quantum wells. *Science*, 314 (5806): 1757–1761.
- [16] König, M., Wiedmann, S., Brüne C., Roth, A. Buhmann, H., Molenkamp, L. W., Qi, X. L. and Zhang, S. C. 2007. Quantum spin hall insulator state in HgTe quantum wells. *Science*, 318 (5851): 766–770.
- [17] van Leuken, H. and de Groot, R. A. 1995. Half-Metallic Antiferromagnets. *Physical Review Letters*, 74 (7): 1171.
- [18] Pickett, W. E. 1998. Spin-density-functional-based search for half-metallic antiferromagnets. *Physical Review B*, 57 (17): 10613.
- [19] Akai, H. and Ogura, M. 2006. Half-Metallic Diluted Antiferromagnetic Semiconductors. *Physical Review Letters*, 97 (2): 026401.
- [20] Ohno, H., Shen, A., Matsukura, F., Oiwa, A., Endo, A. and Iye, Y. 1996. (Ga,Mn)As: A new diluted magnetic semiconductor based on GaAs. *Applied Physics Letters*, 69: 363.
- [21] Tsdirilkovski, I. M. 1996. *Electron Spectrum of Gapless Semiconductors*, edited by Klaus von Klitzing, Springer Series in Solid-State Sciences Vol. 116 (Springer, New York, 1996) and references therein.
- [22] Sheberla, D., Sun, L., Blood-Forsythe, A. M., Er, S., Wade, C. R., Brozek, C. K., Aspuru-Guzik, A. and Dinca, M. 2014. High Electrical Conductivity in $\text{Ni}_3(2,3,6,7,10,11\text{-hexaiminotriphenylene})_2$, a Semiconducting Metal–Organic Graphene Analogue. *Journal of the American Chemical Society*, 136 (25): 8859–8862.
- [23] Lin, T., Shang, X. S., Adisojoso, J., Liu, P. N. and Lin, N. 2013. Steering On-Surface Polymerization with Metal-Directed Template. *Journal of the American Chemical Society*, 135 (9): 3576–3582.

